Kaiser Bessel gridding kernel for seismic data regularization

Akshay Gulati and Robert J. Ferguson

ABSTRACT

The Kaiser Bessel non-uniform Fast Fourier transform (NFFT) kernel balances accuracy and computational cost, and we present an application of this NFFT for seismic trace interpolation. Application of the Bessel kernel for non-uniform samples is not a new algorithm, but it is an approximation scheme that can be used to calculate an approximate spectrum. In one dimension, computational complexity of Kaiser Bessel NFFT is $O(NlogN)$ which is a dramatic improvement from the $O(N^2)$ complexity of the Discrete Fourier transform (DFT), and it is comparable to Fast Fourier transform (FFT). This algorithm can be easily extended to higher dimensions. Least squares is used to refine an approximated spectra followed by simple Inverse Fast Fourier transform (IFFT). The applicability of the proposed method is examined using synthetic seismic data.

INTRODUCTION

During seismic data acquisition, the continuous wavefield is sampled as a discrete wavefield on the survey grid. To reconstruct the continuous wavefield, the spatial sample rate in the inline and crossline directions axis must be selected based on the Nyquist rule (Vermeer, 1990). When this rule is neglected, interpolation is required (Liu and Sacchi, 2004). The quality of the reconstruction directly affects the various steps of data processing processing such as Migration (Spitz, 1991), AVO analysis (Sacchi and Liu, 2005) , imaging (Liu and Sacchi, 2004), and noise removal (Abma and Kabir, 2005) (Soubaras, 1994). Seismic reconstruction algorithms are divided in to two categories: those based on wave equation analysis and those based on Parametric analysis.

Based on a velocity model, wave equation based methods comes under category of a regression approach that use wave propagation to guide reconstruction of the missing samples (Ronen, 1987; Bagaini and Spagnolini, 1999; Stolt, 2002; Trad, 2003; Fomel, 2003; Malcolm et al., 2005; Clapp, 2006; Leggott et al., 2007).

Parametric analysis based reconstruction methods are based on *a priori* information in seismic data, and most are based on the Fourier transform(Schonewille et al., 2003; Liu and Sacchi, 2004; Schonewille et al., 2009; Naghizadeh and Sacchi, 2008b,c, 2009b,a, 2010). The central assumptions are based on the stationarity of the process or based on the fact that most of the power in the power spectrum is concentrated on the lower frequencies, analysis based on this fact known as bandlimitness. Bandlimitness enforces only the use of certain set of frequencies (Feichtinger et al., 1995). These algorithms performs efficiently even in situations where assumptions in not satisfied exactly (Trad, 2008).

Seismic data reconstruction is based on data mapping, generally mapping of spatial domain data to the Fourier domain. The most common bases for obtaining high resolution reconstruction techniques are the Fourier transform (Sacchi et al., 1998; Xu et al., 2005; Liu and Sacchi, 2004; Naghizadeh and Sacchi, 2007b, 2008a, 2009b, 2007a) and the Radon transform (Darche, 1990; Verschuur and Kabir, 1995). In the parabolic Radon transform,

two CMP gathers are combined to improve offset sampling and thus differences between midpoint positions are ignored (Duijndam et al., 1999). Similarly hyperbolic and linear Radon transforms (Thorson and Claerbout, 1985) as well as the parabolic radon transform are suitable for estimating frequencies at irregular nodes, but they suffer aliasing problem due to sparse sampling (Hugonnet and Canadas, 1995), the local Radon transform and the curvelet transform (Hennenfent and Herrmann, 2006b, 2007, 2006a). Another group of signal processing interpolation methods rely on prediction error filtering techniques (Wiggins and Miller, 1972). Spitz (1991) and Porsani (1999) introduce seismic trace interpolation methods using prediction filters. These methods operate frequency-space (f-x) domain. The low frequency in a regular spatial grid are used to estimate the prediction filters needed to interpolate high frequency components. This regular spatial grid make prediction filter methods restricted to regular sampling.

In this paper we introduce the use of Kaiser Bessel window function for the seismic data reconstruction. Combining the window function with Fast Fourier transform will give us the Kaiser Bessel non-uniform Fourier kernel. The need of the non-uniform kernel is based on the constrain that Fast Fourier transform (FFTs) need regular spacing for its application. Non uniform Fast Fourier transforms (NFFT) which are generalizations for the FFT are discussed by many authors in the past (Dutt and Rokhlin, 1993; Steidl, 1998; Duijndam and Schonewille, 1999; Lee and Greengard, 2006). It is important to stress that the Non uniform Fourier kernel is been used for seismic data reconstruction by Duijndam and Schonewille (1999) using B - spline and Gaussian window functions, but Kaiser Bessel window has never been tested. Proposed Kaiser Bessel based Kernel balances between the computational resources and reported to give better result than Gaussian and B- Spline window based kernels, and already been tested in Medical imaging (Knopp et al., 2007).

THEORY

In the case of non-uniform sampling, direct discretization of the forward transformation corresponding to the irregular grid at hand will be highly erroneous. A Better approach will be taking the exact inverse transform from the regularly sampled domain to irregularly sampled domain and use this as a forward model in an inverse problem. The general form can be written in term of matrix vector notation as

$$Am = d, \tag{1}$$

where, A_{mxn} is the forward model, d is the observation vector in time domain consist of true values and m represents Fourier components. Observation vector is irregular sampled spatial value in case of Seismic data reconstruction and finally x is a unknown solution. In Band limited approach, it will always be a over determined problem. General least square solution for such approach will be

$$m = (A^*A)^{-1}A^*d, \tag{2}$$

where A is mapping matrix from one domain to another domain, and A* is its complex conjugate transpose.

This is basic the approach for hyperbolic Radon transform and linear Radon transform by Thorson and Claerbout (1985). If desired, data estimated in the Fourier domain can be transform back to a regular grid in the spatial domain using inverse fast Fourier transform.

Discrete Fourier Transform

The general form of the forward discrete Fourier transform in case of the regular sampling can be defined as

$$\hat{P}_m = \sum_{j=0}^{N-1} P_j e^{-2\pi i n m/N} \quad (m = 0, \cdots, N-1), \tag{3}$$

where P_m are the Fourier coordinates, and P_j is the input signal.

Assuming the regular sampling the transform can be easily inverted as,

$$\hat{P}_j = \sum_{n=0}^{N-1} \hat{P}_m e^{2\pi i n m/N}. \tag{4}$$

Here, $e^{2\pi i n m/N}$ is known as the data mapping kernel. All entries of this data mapping kernel are orthogonal to each other in case of regular sampling.

The forward Discrete Fourier transform (DFT) for regularly sampled seismic data (Duijndam et al., 1999) can be written to include sample spacing as

$$\hat{P}(k_x, \omega) = \Delta x \sum_{n=0}^{N-1} P(n\Delta x, \omega) e^{-ink\Delta x}, \tag{5}$$

where ω is the temporal frequency, Δx is sample interval in spatial domain and k_x is the wave number. Regular sampling in the spatial domain enforces periodicity.

In Equation 5, to avoid aliasing after the Fourier transform, it is required to keep Δx small. For avoiding aliasing and maintaining economics of seismic survey, it is always better to restrict the sampling based on Shannon sampling theory. DFT is the mapping of N point signal $(x_1, x_2, \cdots x_N)$ in to N Fourier coefficients X_K. In matrix vector form the DFT can be denoted as

$$X = DFT * x, \tag{6}$$

where DFT is the Fourier kernel. From equation 6, DFT is a Fourier Matrix that maps N dimensional vector x in to another N dimensional vector X. To transform back to the spatial domain, we need DFT^{-1}, which is inverse DFT Matrix. The Inverse discrete Fourier Transform is defined by

$$P(x, \omega) = \frac{\Delta k}{2\pi} \sum_{m=-M}^{m=M} \hat{P}(m\Delta k, \omega) e^{-im\Delta kx}, \tag{7}$$

where Δk is the sampling interval in Fourier domain, $N = 2M + 1$, and $\Delta k = \frac{2\pi}{N\Delta x}$. The matrix vector form of Equation 7 is

$$x = DFT^H * X, \tag{8}$$

where DFT^H is the Hermitian adjoint of the DFT. Since sampling is regular, $DFT_{N \times N}$ is orthogonal, which implies

$$DFT^H * DFT = NI_N, \tag{9}$$

where I_N is an N dimensional identity matrix. Equation 9 shows that DFT is an orthogonal transformation, and that the inverse is computed using a Hermitian operator. The cost of inverting $N \times N$ Hermitian operator is $O(N^2)$ instead of $O(N^3)$. Cost is further diminished to $O(NlogN)$ using the fast Fourier transform (FFT) instead of matrix vector multiplication. However, FFT can't be applied in the case of irregular sampling

$$DFT^H * DFT \neq NI_N, \tag{10}$$

Equation 10 shows that when sampling is irregular, its not simple to invert the DFT matrix, since columns of the DFT matrix are no longer orthogonal. The approximation converging closest to DFT for irregular sampling is the weighted Fourier Transform (DFT)

$$P(m\Delta k, \omega) = \sum_{n=0}^{N-1} P(x_n, \omega)e^{jm\Delta k x_n}\Delta x_n, \tag{11}$$

where Δk is the regular sample interval in Fourier domain. x_n represents the positions of the irregular nodes, and Δx_n is the weighting factor which depends upon the distance between the samples in spatial domain according to

$$\Delta x_n = \frac{x_{n+1} - x_{n-1}}{2}, \quad n = 0, \cdots, N-1. \tag{12}$$

The DFT in Equation 11, however, is not a unitary transformation, as it fails the dot product test (i:e the dot product of two vectors before the transformation should be equal to dot product after the transformation). For this reason, it is not possible to reconstruct the original domain by a simple inverse FFT (IFFT).

Feichtinger et al. (1995) suggests an approach to handle the irregular grid problem by putting a band limitation restrain on the data. If Δk is the sampling interval in Fourier domain than the data is band limited to between $[-M\Delta k, M\Delta k]$. Accordingly, Equation 4 for N irregular samples $(x_0, x_1 \cdots, x_{N-1})$ can be denoted in matrix vector notation as

$$y = A\hat{p}, \tag{13}$$

where,

$$y_n = P(x_n, \omega), \tag{14}$$

y_n represents the values on the non-uniform grid,

$$\hat{p}_m = \hat{P}(m\Delta k, \omega), \tag{15}$$

and

$$A_{nm} = \frac{\Delta k}{2\pi}e^{-jm\Delta k x_n}, \tag{16}$$

where $\hat{p}_m$ is the solution for the linear least square problem, and A_{nm} is the data mapping kernel. However, real data is never band limited; there will always be some spatial frequencies above the restricted bandwidth. It can be treated as noise in the forward model and can be included in Equation 13 as

$$y = A\hat{p} + Noise. \tag{17}$$

Further, $\hat{p}$ can be estimated by

$$\hat{p} = \left(A^H W A + k^2 I\right)^{-1} A^H W y, \tag{18}$$

where W is a weight matrix, k is the stabilization factor, and A^H is the complex conjugate transpose of A. From equation's 14, 15, and 16, the last term of equation 18 can be written as

$$A^H W y = \frac{\Delta k}{2\pi} \sum_{n=0}^{N-1} P(x_n, \omega) e^{jm\Delta k x_n} W_{nn}, \tag{19}$$

where $W_{nn} = \Delta x_n$. Here, except for constant $\frac{\Delta k}{2\pi}$, equation 19 is equivalent to equation 11, which represents weighted DFT. Estimated Fourier spectrum $\hat{p}$ can be transformed back to the spatial domain by direct inverse transform. The DFT is a major computational task for the forward transform, as computational complexity of the DFT is $O(N^2)$. Many inversion schemes that are use in data processing Sacchi et al. (1998); Sacchi and Ulrych (1996) rely on the solution of normal equations the right hand side of which is DFT.

The Kaiser Bessel kernel is a solution that can replace slow DFT with faster algorithm. Fast algorithm will make many algorithms where DFT is used as practical for industry.

METHODOLOGY

Methodology is divided in to two categories Forward problem and Inverse Problem. Both is calculated using NFFT Kaiser Bessel Kernel. Methodology can be divided in Following steps

1. $A^H W y = b$, calculates direct forward transform using NFFT kernel.

2. $U = (A^H W F + k^2 I)$ is the deconvolution operator using NFFT and adjoint NFFT kernels.

3. $U\tilde{A} = b$, calculates least squares system for $\tilde{p}$.

4. $y = IFFT(\tilde{p})$ calculates direct backward transform on regular grid using Fast IFFT.

Forward problem

The non-uniform Fast Fourier gridding algorithm can be numerically expressed in following steps: gridding, FFT, deconvolution. The gridding is obtained by convolution of the sampled signal values with a convolution function followed by re-sampling onto a Cartesian grid. Convolution with Kaiser Bessel function $kb(x)$ is carried out to make the signal approximately band-limited according to

$$p_g(m) = kb(x) * p(x), \tag{20}$$

where $p_g(m)$ is the result of spatial convolution. Equation 20 can be written as multiplication in the Fourier domain as

$$P_g(m) = KB(m) \times P(m), \tag{21}$$

where $P_g(m)$ is the Fourier spectrum of $p_g(m)$ in Fourier domain. For efficiency Kaiser Bessel need to be truncated, thus generating n samples for $p_g(m)$ where

$$n = -int\left(\frac{q+1}{2}\right) + 1, \cdots, N + int\left(\frac{q+1}{2}\right) - 1, \tag{22}$$

and where $int(x)$ truncates to the largest integer smaller than x for $x \geq 0$. The algorithm is initialized at $p_{\tilde{g}}(n) = 0$, where subscript $\tilde{g}$ indicates we apply a Kaiser Bessel filter and keep updating by summation of the N shifted filters. This summation of N shifted filter can be given by

$$p_{\tilde{g}}(n) \leftarrow p_{\tilde{g}}(n) + \Delta x p_n kb(n\Delta x - x_n). \tag{23}$$

Equation 23 for spreads the irregular samples on to a regular grid. The sampling $p_{\tilde{g}}(n) = \Delta x p_1(n\Delta x)$ is similar to equation 24 in Fourier domain which can be written as

$$P_g(m) = \sum_{I \in Z} P(m + IN) KB(m + IN). \tag{24}$$

When $P_g(m)$ is broadband, aliasing will occur when $KB(m + IN) \neq 0$ for any $I \neq 0$. It is suggested by (Duijndam and Schonewille, 1999) that to remove the aliasing, there is requirement of making the signal periodic according to

$$p_{\tilde{g}}(n) = \sum_{I=-\infty}^{\infty} p_{\tilde{g}}(n + IN), \ \ n = 0, 1, 2, \cdots, N - 1, \tag{25}$$

where $p_{\tilde{g}}(n + lN) = 0$ is outside the interval given by equation 22. Convolution of the signal followed by the discrete transform can be represented by

$$P_g(m)_{FFT} = \sum_{n=0}^{N-1} p_{\tilde{g}}(n) e^{j2\pi nm/N}, \ \ m = \frac{N}{2}, \cdots, \frac{N}{2} - 1, \tag{26}$$

where $P_g(m)_{FFT}$ is the spectrum obtained using the FFT. Finally correction for convolution is carried out by deconvolution in the Fourier domain according to

$$P(m) = \frac{P_g(m)_{FFT}}{KB(m)}, \tag{27}$$

where $P(m)$ is the approximate spectrum, and $KB(m)$ is the spectrum obtained by equation's 11 and 27.

Window function

NFFT algorithms are based on convolution of sampled signal with a band limiting filter, and several different names are indicated in the literature. Jackson et al. (1991) discuss these algorithms in terms of image processing and refer to them as griding algorithms. Beylkin et al. (1991) proposes a similar as the irregular Fourier transform algorithm where convolution with B-spline is carried out to make the signal approximately band limited. Jackson et al. (1991) discuss several forms of filters which can be used, and a truncated Gauss filter is introduced by Dutt and Rokhlin (1993).

Most of the recent development in these algorithms deals with optimization of above windows functions, but still Kaiser Bessel window function gives best result (Knopp et al., 2007).

Kaiser Bessel window function

Prolate Spheroidal wave function (PSWF) have finite time support and maximum concentration of Energy within a given bandwidth. The closet window function which provides good approximation is Kaiser Bessel function. The PSWF is the eigenfunction having the largest eigenvalue of the operation of repeatedly low-pass filtering a function and bandlimiting it. It is difficult to compute but the Kaiser-Bessel function is a close approximation of the PSWF. For a given filter $q\Delta x$ and Bandwidth B, the least amount of energy outside desired passband i:e minimization of

$$\frac{\int_{|m|>B}|\tilde{g}(m)|^2 dm}{\int_{\infty}^{\infty}|\tilde{g}(m)|^2 dm}. \tag{28}$$

The Kaiser Bessel function can be represented as Knopp et al. (2007)

$$g(x) = \frac{1}{q\Delta x}I_o\beta\sqrt{1-\left(\frac{2x}{q\Delta x}\right)^2} \quad \frac{-q\Delta x}{2} \leq x \leq \frac{q\Delta x}{2}, \tag{29}$$

where I_o is the zeroth order modified Bessel function of its first kind. In Frequency domain, its Fourier transform is used for deconvolution purpose. Fourier domain representation of Kaiser Bessel function

$$\tilde{g}(m) = \frac{sin(\sqrt{\pi^2(q(\Delta x)^2 m^2 - \beta^2)})}{\sqrt{\pi^2(q(\Delta x)^2 m^2 - \beta^2)}}. \tag{30}$$

Figure 2a represents Kaiser Bessel window for various value of β in spatial domain. β is the parameter for Kaiser window, which gives control over trade off between mainlobes width and sidelobes level. Large β gives wider main lobe but lower side lobes as shown in Figures 2a and 2b. For maximum frequency resolution, always narrowest main lobe is preferred. Jackson et al. (1991) carried out detailed analysis of the various convolution functions leading to the approximation for the prolate spheroidal function. Different value of β is suggested for 30 in (Jackson et al., 1991). For all calculation purpose value of q is taken as 6 and value of $\beta = 2$. These values are taken as a optimum by Knopp et al. (2007).

Inversion

In general the linear system we will solve in this problem, so the solution can only be approximated up to a residual of the form

$$r = y - A\tilde{p}. \tag{31}$$

In order to compensate for the missing samples it is important to incorporate a weight function W, $W > 0$ and the problem becomes a

$$argmin||y - A\tilde{p}||_W^2 = \sum_{j=0}^{M-1} w_j|y_j - f(x_j)|2 \rightarrow min, \tag{32}$$

where W $=diag(w_j)_{j=0,\cdots,M-1}$.

EFFICIENCY

The problem of regularization in the least squares NFFT framework is divided in two categories: forward method and inversions. The Direct forward transform is been computed using NFFT which is A^H and for the inversion purpose operator $U = (A^H W A + k^2 I)$ is computed. For computing the inversion operator, the forward Fourier kernel A^H and its adjoint A is already computed using NFFT. It has already been that NFFT give a computational advantage over DFT. Further more iterative solution of 32 has been analysis in detail in large number of papers (Feichtinger et al., 1995). The adaptive weights conjugate gradient Toeplitz method (ACT) applies the conjugate gradient method to the weighted normal equation which can be written as

$$A^H W A \tilde{p} = A^H W y. \tag{33}$$

SYNTHETIC TESTS

Purpose of any reconstruction algorithm can only be solved if it is tested as general algorithm. Its important stress that not all the methods are capable of dealing with regular as well as irregular sampling. In fact, most of the Parametric signal reconstruction technique fails to deal with irregular sampling (Naghizadeh and Sacchi, 2008b,c, 2009b; Hennenfent and Herrmann, 2008, 2007).

Synthetic 1D examples

Figure 1 demonstrates effect of the sampling on seismic data. Synthetic hyperbolic events (Figure 1a) and its Fourier domain representation (Figure 1b). In case of regular decimation (Figure 1d), strong coherent noise (Figure 1d) will be created due to acquisition. Noise is highly structured with strong amplitudes. Most of the regular interpolation techniques is based on the idea of using non aliased low frequency and de-alias higher frequency. Abma and Kabir (2005) pointed out that most interpolation method based on regular sampling whereas irregular sampling generate weak noise. In irregular sampling (Figure 1e), Power is focused at few Fourier coefficients and noise is spread whole transform domain (Figure 1f). Sparser the signal, straightforward will be the reconstruction.

For examining the performance of Kaiser Bessel NFFT algorithm with various sampling operators, we created a simple sin signal in Figure 3 as well as another signal in Figure 4 which is composed of two harmonics. Detailed analysis with varying gaps, extrapolation, random sampling and uniform sampling is carried out.

For 1 dimension examples we will take case of simple sinusoidal with 256 samples, at sampling rate of 10ms. Top panel will show the Decimated spatial domain and panel below it is reconstructed missing samples. Figure 3a shows the the 30 % randomly decimated signal and reconstructed sinusoidal. Even with 50% randomly decimation in Figure 3b algorithm seems to do pretty well. On implementing high decimation sampling functions of 60% in Figure 3c results are good, all missing samples have been successfully reconstructed. On going further decimation in Figure 3d due to lost of the Fourier coefficients its is not able to recons truct the same amplitude back, except at one point where it is missing

most of the samples.

Gaps

In the previous test, it is observed that algorithm fails some time when more number of Fourier coefficients are missing from a single location. This behaviour is further tested in gap test. In this different gaps will be created by taking more number of Fourier coefficients from a single location. Algorithm is tested for all size of gaps. Input signal composed of two harmonics , with sampling interval of 10ms for 256 samples. In the case of small gaps in Figure 4b, reconstruction is perfect. Even in the presence of large gaps in Figure 4d, algorithm works effectively.

Extrapolation

Extrapolation test is done for the reconstruction algorithm, purpose of algorithm is to extrapolate the missing samples. Extrapolation is been tested on combination of two harmonics for two categories, small gaps and large gaps in Figures 4e and 4g. Reconstructed extrapolated harmonics can be seen in Figures 4f and 4h. Algorithms can easily handle the stationary harmonics with large gaps. Algorithm can also be applied on simple non stationary harmonics when taken small windows, and events are assumed to be stationary.

SYNTHETIC 2D EXAMPLES

In the case of 2D data reconstruction, the Fourier reconstruction is iterative on each frequency slice in fk domain. NFFT least square will be applied on each frequency slice, with iteratively moving to next slice. In Figure 5, there are three seismic events with different dips and amplitudes. The seismic wavelet is Ricker wavelet with peak frequency of 50 Hz. Sampling rate for seismic data acquisition is 4ms. Figure 5 is the an original synthetic section. Figure 6 represents Fourier domain representation for original section. Before testing algorithm for heavy decimation operators, its been tested for 10% random decimation in Figure 6. NFFT Least squares works perfectly in Figures 5 and 6 for the small random decimation.

Randomly decimated Dipping Events

Random sampling in the spatial domain (Figure 7a) can result in low amplitudes artifact like in Figure (7c) along with the original Fourier events. The artifacts are the resultant of random sampling operator which is 50% resultant due to decimation in original data in Figure 7a. Reconstructed data in Figure 7b in case of 50% random decimation is as good as original. Figure 7b proves that algorithm works for the seismic section with half of the missing samples. Even Fourier domain in Figure 7c shows all the energy concentrated on the dipping events, with no energy getting dissipated.

Further moving to higher decimation of 80% in 7e low amplitudes artifacts are more dominant. Along with the dominant artifacts, aliasing for the dips can be seen in Figure 7g. Noisy artifacts are observed in Figure 7f as compared to Figure 7f, its because of the big gap in Figure 7e. It was seen before that algorithm works for big gaps in case

of simple harmonics in Figures (4b, 4d), but it is effective even in case of linear dipping events. Its important to test when algorithm fails for knowing its limitation. Therefore final data is tested using random sampling operators of 80% decimations in Figure7f. Figure 7e shows 80% decimated data, with its Fourier domain in Figure 7g. It should be notice that Fourier domain of 80% decimation in Figure 7g has more aliased events than with 50% decimation, its again due to the presence of more gaps in the decimated section in Figure 7e as comparison to 50% decimation in Figure 7a. Algorithm started to fails with 80% decimation as seen in reconstructed section in Figures 7f, there are low amplitudes artifacts in the recovered Fourier domain (Figure 7h) as well. Events in recovered section are still well defined (Figure 7f) but with the high amplitude noise in the section. Both reconstructed, t-x domain and f-k domain in Figure 7f and Figure 7h demonstrates the limitation of the algorithm.

Uniform decimation for dipping Events

In order to generalize the algorithm for the interpolation, we will be testing it with the uniformly decimation operators. Parametric reconstruction technique seems not to perform very well, when implemented on the uniformly decimated seismic section. In case of uniform decimation, replicas of events are created in the Fourier domain which is difficult to separate. But with the band-limiting approach like Least square NFFT, replicated spectrum of event can be isolated in the low frequency of data. It is because of the higher power spectrum at low frequencies. Uniform decimation factors of 2 in Figure 8a and 4 in Figure 8e are implemented.

2D Synthetic section is decimated by a factor 2 in Figure 8a. Exact replicas of planar and dipping events are created in FK domain of Figure 8c. Reconstructed data in Figure 8b and its Fourier domain in Figure 8d is recovered. On increasing the decimation factor to 4 in Figure 8e, we have more replicas of planar and dipping events in Figure 8h as compare to 8d. But the recovered data in Figure 8f has well define events like in Figure 8f, setting reputation of algorithm to work on uniformly decimated data as well. Further for uniform sampling, like random sampling there is need of minimum number of samples so that algorithm can recover the data.

Hyperbolic events

In case of hyperbolic events in Figure 9, data can always be windowed thus assuming that events are linear. But, we already seen the application of LS-NFFT on linear events. Applying LS-NFFT on the decimated data without windowing in Figure 9a. In upper part of reconstructed data in Figure 9b apexes are successfully reconstructed. But still some high amplitude noise is observed.

CONCLUSIONS

Low computational cost of LS-NFFT make it a robust and practical algorithm. This method successfully reconstruct the missing samples. This algorithm is effective both in case of random sampled data as well as uniform sampling. Algorithm can be easily extended to higher dimensions, and it will prove to be cost effective even for it. Though it

is able to reconstruct the curved events. But a good windowing strategy which enforces linearity for curved events will sure provide better results in that case. NFFT and Adjoint NFFT is a strong tool and can be use as a effective tool in other seismic processing steps.

REFERENCES

Abma, R., and Kabir, N., 2005, Comparison of interpolation algorithms: The Leading Edge, **24**, No. 10, 984–989.

Bagaini, C., and Spagnolini, U., 1999, 2-d continuation operators and their applications: Geophysics, **64**, No. 2, 524–538.

Beylkin, G., Coifman, R., and Rokhlin, V., 1991, Fast wavelet transforms and numerical algorithms: Comm. on Pure and Appl. Math., **44**, 141–183.

Clapp, R. G., 2006, Amo inversion to a common azimuth dataset: SEG, Expanded Abstracts, **25**, No. 1, 2097–2101.

Darche, G., 1990, Spatial interpolation using a fast parabolic transform: 60th Annual International Meeting, SEG, Expanded Abstarcts, 1647–1650.

Duijndam, A. J. W., and Schonewille, M., 1999, Nonuniform fast fourier transform: Geophysics, **64**, 551.

Duijndam, A. J. W., Schonewille, M. A., and Hindriks, C. O. H., 1999, Reconstruction of band-limited signals, irregularly sampled along one spatial direction: Geophysics, **64**, No. 2, 524–538.

Dutt, A., and Rokhlin, V., 1993, Fast fourier transforms for nonequispaced data: SIAM J. Sci. Comput., **14**, No. 6, 1368–1393.

Feichtinger, H. G., Grochenig, K., and Strohmer, T., 1995, Efficient numerical methods in non-uniform sampling theory: Numerische Mathematik, **69**, 423–440.

Fomel, S., 2003, Seismic reflection data interpolation with differential offset and shot continuation: Geophysics, **68**, No. 2, 733–744.

Hennenfent, G., and Herrmann, F. J., 2006a, Application of stable signal recovery to seismic data interpolation: 76th Annual International Meeting, SEG, Expanded Abstarcts, 2797–2801.

Hennenfent, G., and Herrmann, F. J., 2006b, Seismic denoising with nonuniformly sampled curvelets: IEEE Trans. on Computing in Science and Engineering, **8**, No. 3, 16–25.

Hennenfent, G., and Herrmann, F. J., 2007, Random sampling: new insights into the reconstruction of coarsely-sampled wavefields: 77th Annual International Meeting, SEG, Expanded Abstarcts, 2575–2579.

Hennenfent, G., and Herrmann, F. J., 2008, Simply denoise: Wavefield reconstruction via jittered undersampling: Geophysics, **73**, No. 3, V19–V28.

Hugonnet, P., and Canadas, G., 1995, Aliasing in the parabolic radon transform: SEG Expanded Abstracts, **85**, No. 1, 1366–1369.

Jackson, J. I., Meyer, C. H., Nishimura, D. G., and Macovski, A., 1991, Selection of a convolution function for Fourier inversion using gridding [computerised tomography application]: Medical Imaging, IEEE Transactions on, **10**, No. 3, 473–478.

Knopp, T., Kunis, S., and Potts, D., 2007, A note on the iterative mri reconstruction from nonuniform k-space data: Int. J. Biomed. Imag., **2007**, Article ID 24,727, 9 pages.

Lee, J., and Greengard, L., 2006, The type 3 nonuniform fft and its applications: Journal of Computational Physics, **206**, 1–5.

Leggott, R. J., Wombell, R., Conroy, G., Noss, T., and Williams, G., 2007, An efficient least-squares migration: 69th EAGE Conference and Exhibition, Expanded Abstracts, P178.

Liu, B., and Sacchi, M. D., 2004, Minimum weighted norm interpolation of seismic records: Geophysics, **69**, No. 6, 1560–1568.

Malcolm, A. E., Hoop, M. V. d., and LeRousseau, J. H., 2005, The applicability of dip moveout/azimuth moveout in the presence of caustics: Geophysics, **70**, No. 1, S1–S17.

Naghizadeh, M., and Sacchi, M. D., 2007a, Multistep autoregressive reconstruction of seismic records: Geophysics, **72**, No. 6, V111–V118.

Naghizadeh, M., and Sacchi, M. D., 2007b, Reconstruction of irregularly sampled, aliased data with multistep autoregressive operators: SEG Technical Program Expanded Abstracts, **26**, 2580–2583.

Naghizadeh, M., and Sacchi, M. D., 2008a, Sampling functions and sparse reconstruction methods: EAGE Conference, Rome, Italy.

Naghizadeh, M., and Sacchi, M. D., 2008b, Seismic data reconstruction using multidimensional prediction filters: EAGE Conference, Rome, Italy.

Naghizadeh, M., and Sacchi, M. D., 2008c, Seismic trace interpolation using adaptive prediction filters: CSEG Annual meeting.

Naghizadeh, M., and Sacchi, M. D., 2009a, Robust reconstruction of aliased data using autoregressive spectral estimates: EAGE Conference, Amsterdam, Netherlands.

Naghizadeh, M., and Sacchi, M. D., 2009b, Sampling considerations for band-limited fourier reconstruction of aliased seismic data: EAGE Conference, Amsterdam, Netherlands.

Naghizadeh, M., and Sacchi, M. D., 2010, Seismic data reconstruction using multidimensional prediction filters: Geophysical Prospecting, **58**, No. 2, 157–173.

Porsani, M., 1999, Seismic trace interpolation using half-step prediction filters: Geophysics, **64**, No. 5, 1461–1467.

Ronen, J., 1987, Wave-equation trace interpolation: Geophysics, **52**, No. 7, 973–984.

Sacchi, M., and Liu, B., 2005, Minimum weighted norm wavefield reconstruction for ava imaging: Geophysical Prospecting, **53**, No. 6, 787–801.

Sacchi, M. D., and Ulrych, T. J., 1996, Estimation of the discrete fourier transform, a linear inversion approach: Geophysics, **61**, No. 4, 1128–1136.

Sacchi, M. D., Ulrych, T. J., and Walker, C. J., 1998, Interpolation and extrapolation using a high-resolution discrete fourier transform: IEEE Transaction on Signal Processing, **46**, No. 1, 31–38.

Schonewille, M., Klaedtke, A., Vigner, A., Brittan, J., and Martin, T., 2009, Seismic data regularization with the anti-alias anti-leakage fourier transform: First Break, **27**, 85–92.

Schonewille, M. A., Romijn, R., Duijndam, A. J. W., and Ongkiehong, L., 2003, A general reconstruction scheme for dominant azimuth 3d seismic data: Geophysics, **68**, No. 6, 2092–2105.

Soubaras, R., 1994, Signal-preserving random noise attenuation by the f-x projection: 64th Annual International Meeting, SEG, Expanded Abstarcts, 1576–1579.

Spitz, S., 1991, Seismic trace interpolation in the *F-X* domain: Geophysics, **56**, No. 6, 785–794.

Steidl, G., 1998, A note on fast fourier transforms for nonequispaced grids: Advances in Computational Mathematics, **9**, 337–352, 10.1023/A:1018901926283.
URL http://dx.doi.org/10.1023/A:1018901926283

Stolt, R. H., 2002, Seismic data mapping and reconstruction: Geophysics, **67**, No. 3, 890–908.

Thorson, J. R., and Claerbout, J., 1985, Velocity-stack and slant-stack stochastic inversion: Geophysics, **50**, No. 6, 2727–2741.

Trad, D., 2003, Interpolation and multiple attenuation with migration operators: Geophysics, **68**, No. 6, 2043–2054.

Trad, D., 2008, Five dimensional seismic data interpolation: 78th Annual International Meeting, SEG, Expanded Abstarcts, 978–981.

Vermeer, G., 1990, Seismic wavefield sampling, vol. 4: Society of Exploration Geophysicsits, Tulsa, OK.

Verschuur, D. J., and Kabir, M. M. N., 1995, Restoration of missing offsets by parabolic radon transform: Geophysical Prospecting, **43**, No. 3, 347–368.

Wiggins, R. A., and Miller, S. D., 1972, New noise-reduction technique applied to long-period oscillations from the alaska earthquake: Bull. Seism. Soc. Am., **62**, 471–479.

Xu, S., Zhang, Y., Pham, D., and Lambare, G., 2005, Antileakage fourier transform for seismic data regularization: Geophysics, **70**, No. 4, V87–V95.
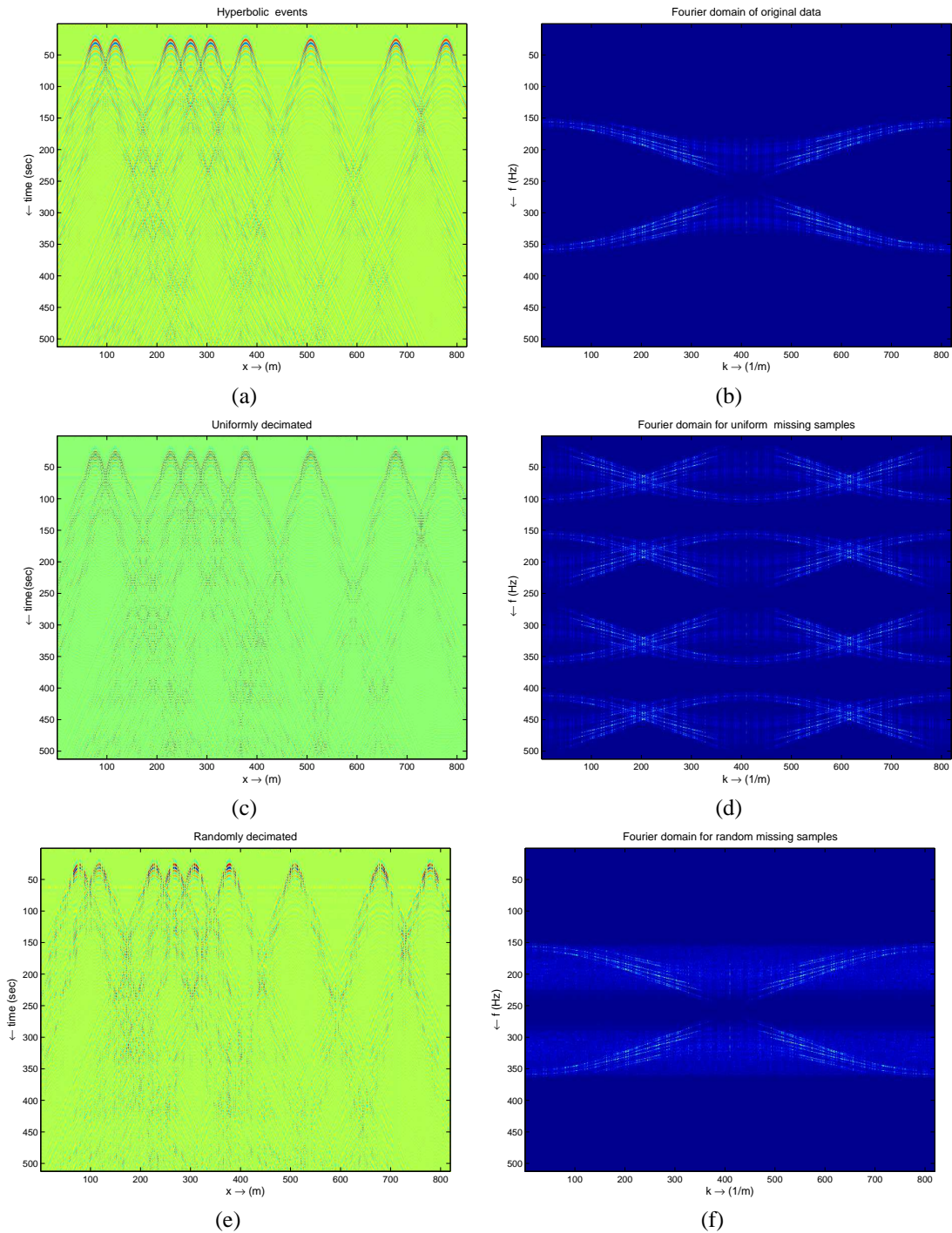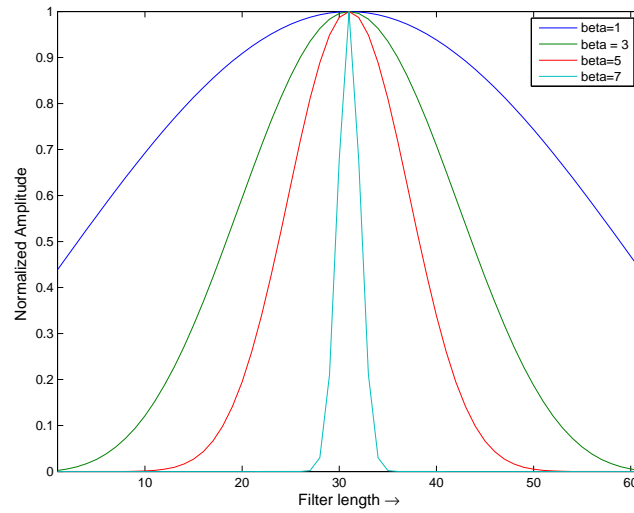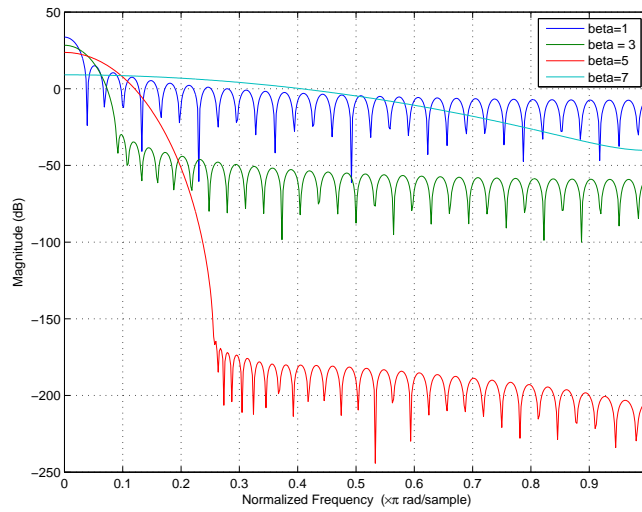
FIG. 1: Effect of sampling on Seismic data. a) Hyperbolic events in spatial domain. b) Fourier domain for Hyperbolic events. c) Uniform decimation for Hyperbolic events. d) Fourier domain for uniformly missing samples. e) Random decimation for Hyperbolic events. f) Fourier domain for Randomly missing samples.

(a)

(b)

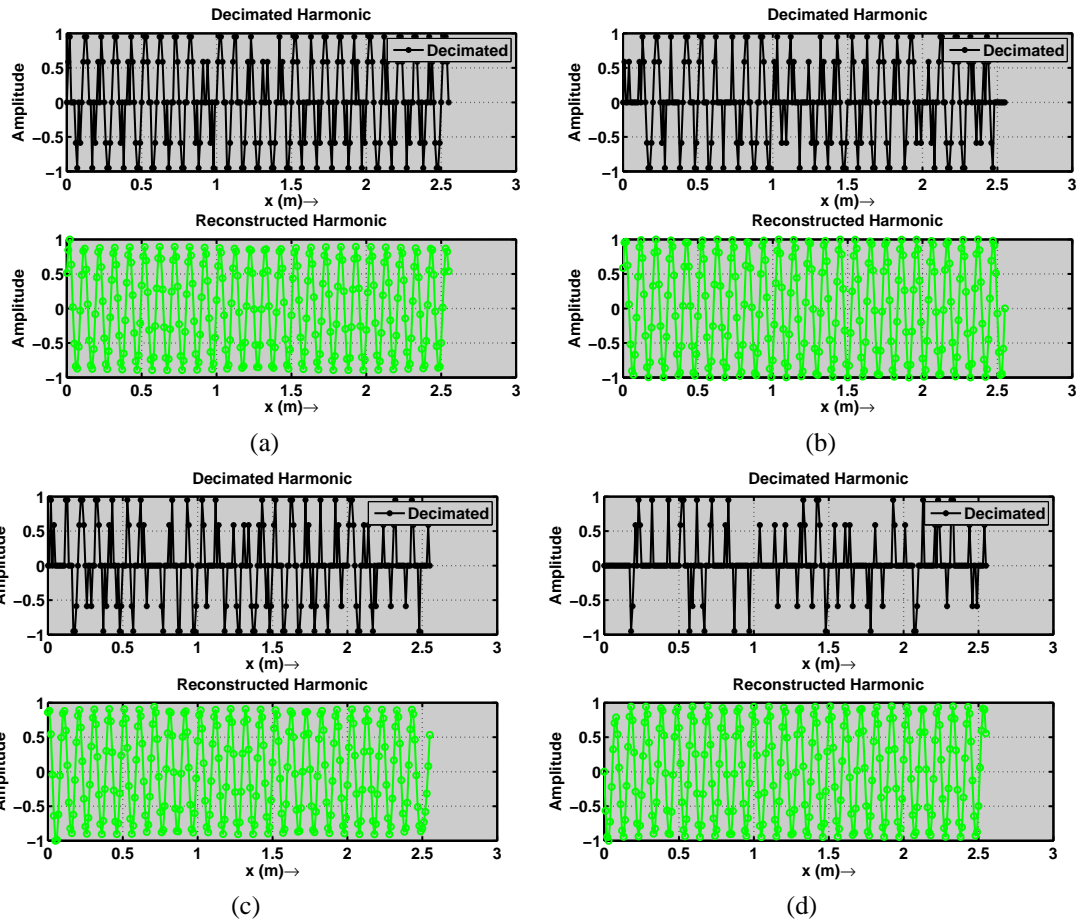FIG. 2: Kaiser Bessel filter. a) Kaiser window in spatial domain. b) Kaiser window in Fourier domain.

FIG. 3: Reconstruction for Harmonics. a) Harmonics with 30 % decimation. b) Harmonics with 50 % decimation. c) Harmonics with 60 % decimation. d) Harmonics with 80 % decimation.
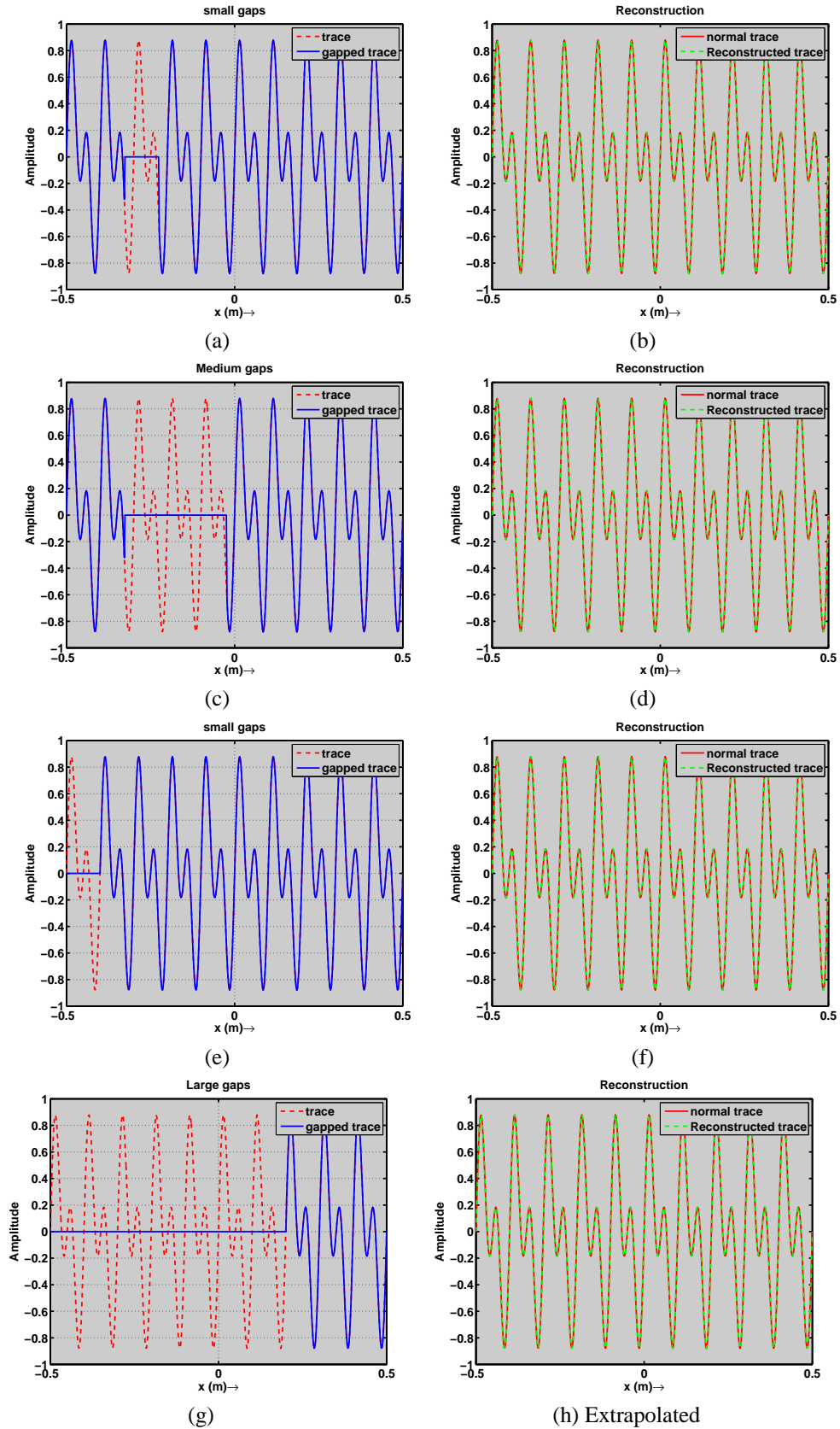
FIG. 4: Reconstruction and extrapolation of Gaps. a) Small size gaps. b) Reconstructed small gaped harmonic. c) Medium size gaps. d) Reconstructed medium gaped harmonic. d) Small side gaps. e) Extrapolated small gaps. f) Big side gaps. g) Extrapolated big gaps.
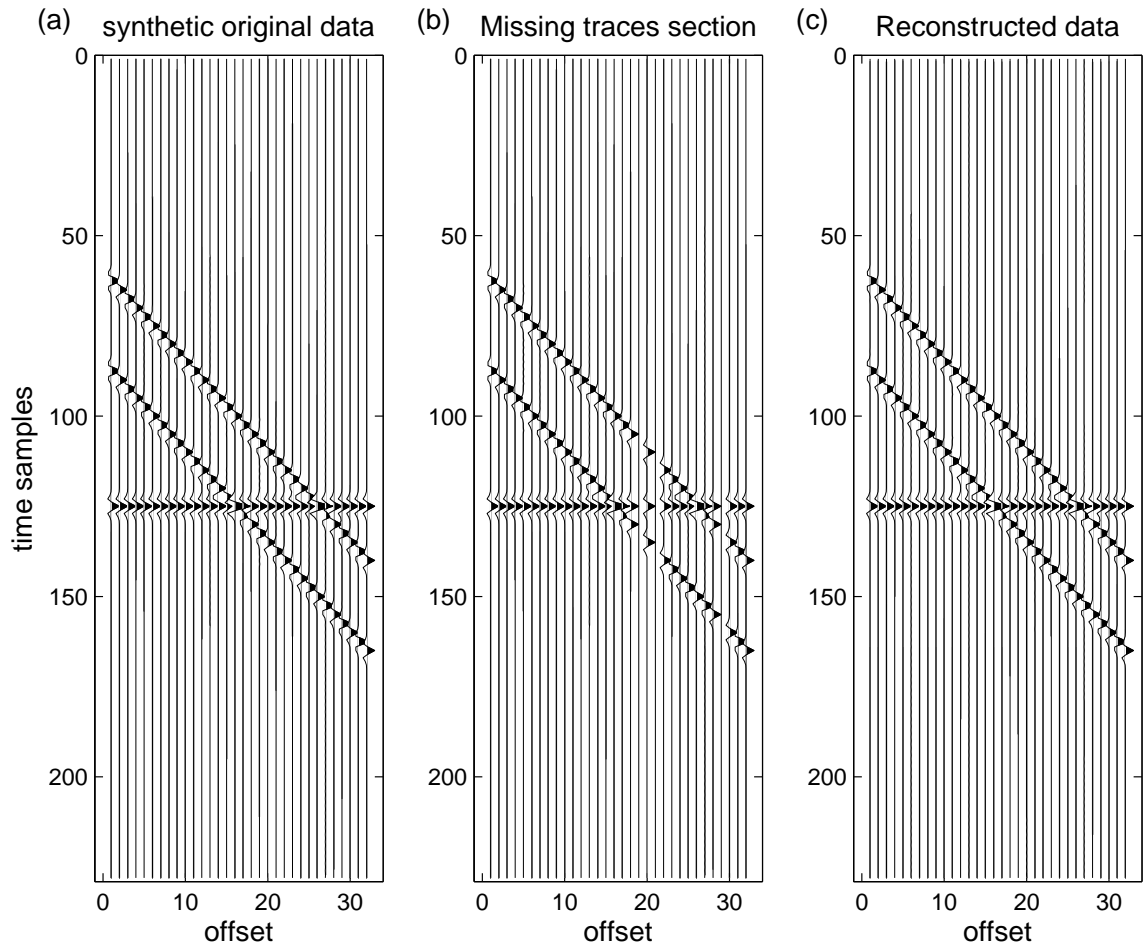
FIG. 5: Synthetic seismic data. a) Synthetic original data. b) Missing traces section with 10 % decimation. c) Reconstructed traces for synthetic data.
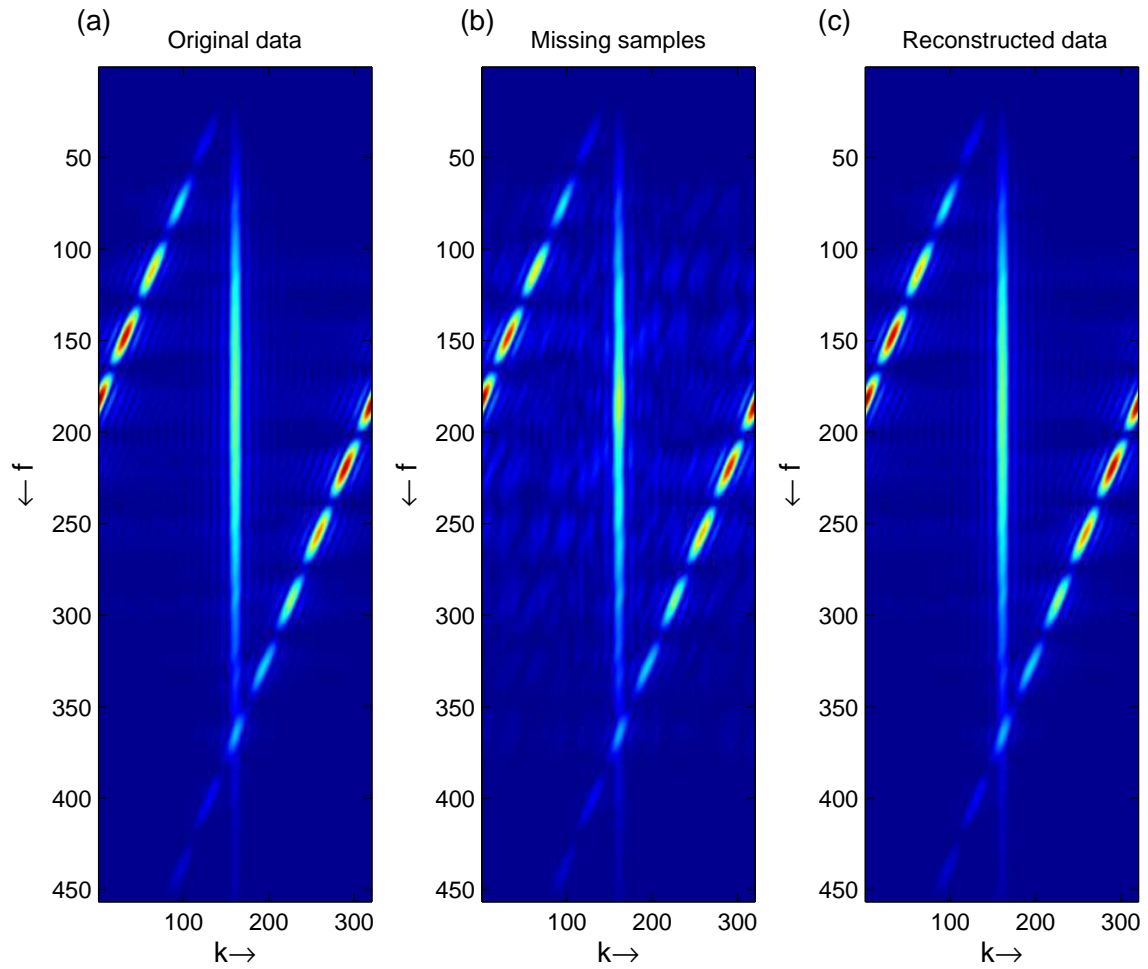
FIG. 6: Fourier domain representation. a) Fourier domain for original data. b) Fourier domain for missing traces with 10 % decimation. c) Fourier domain for reconstructed data. of original event with 10 % decimated data and reconstructed data.
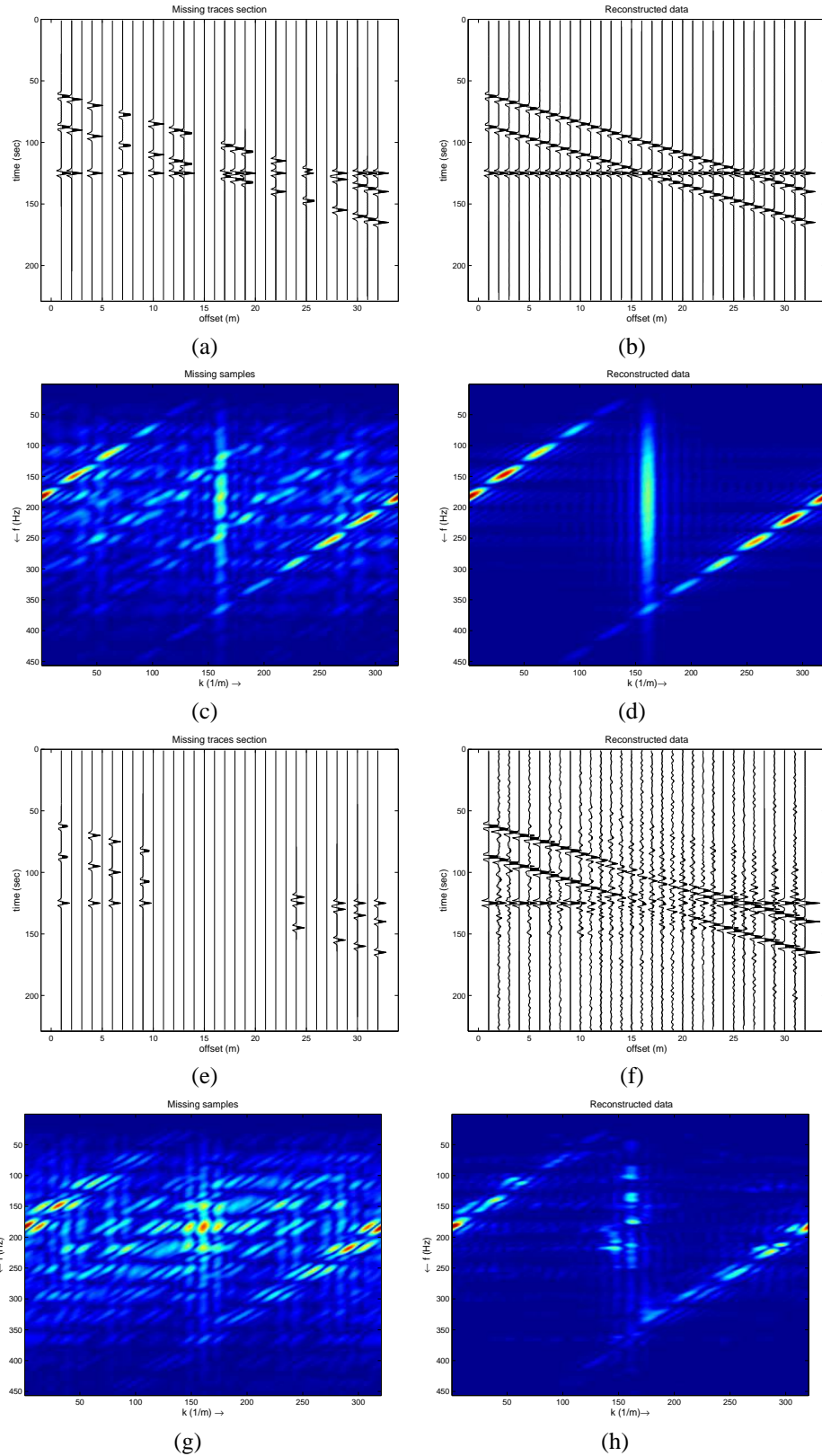
FIG. 7: Reconstruction of random sampled Seismic data. a) 50 % Decimated data. b) Reconstructed data for 50 % decimated data. c) Fourier domain for 50 % decimated data. d) Fourier domain for Reconstructed data with 50% decimation . e) 80 % Decimated data. f) Reconstructed data for 50 % decimated data. g) Fourier domain for 80 % decimated data. h) Fourier domain for Reconstructed data with 80% decimation.
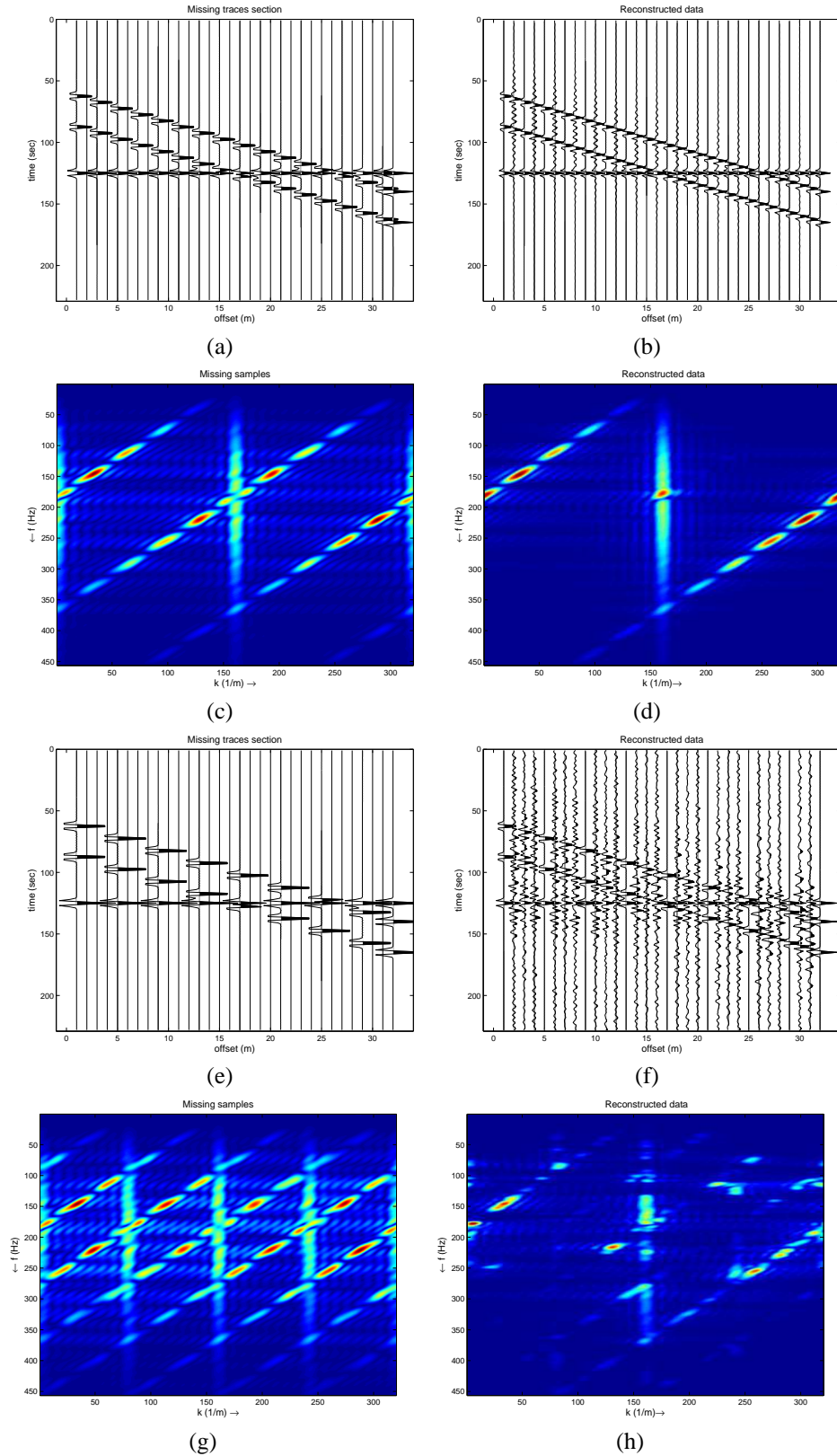
(a)

(b)

(c)

(d)

(e)

(f)

(g)

(h)

FIG. 8: Reconstruction of uniformly sampled seismic data. a) Decimation by factor of 2. b) Reconstructed data. c) Fourier domain for decimation by factor of 2. d) Reconstructed data in Fourier domain for factor of 2 decimation. e) Decimation by factor of 4. f) Reconstructed data. g) Fourier domain for decimation by factor of 4. g) Reconstructed data in Fourier domain for factor of 4 decimation.
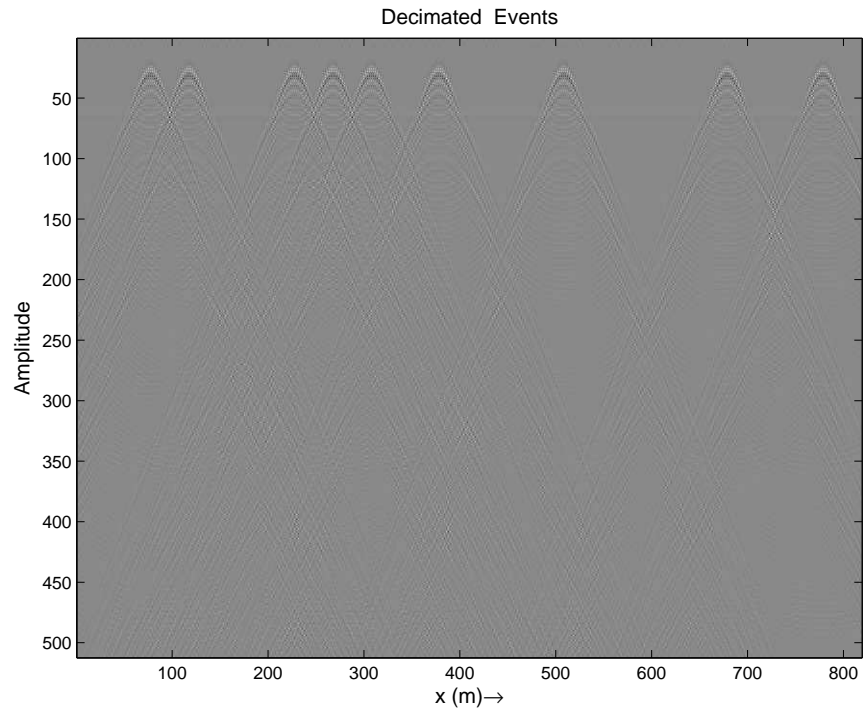
(a)
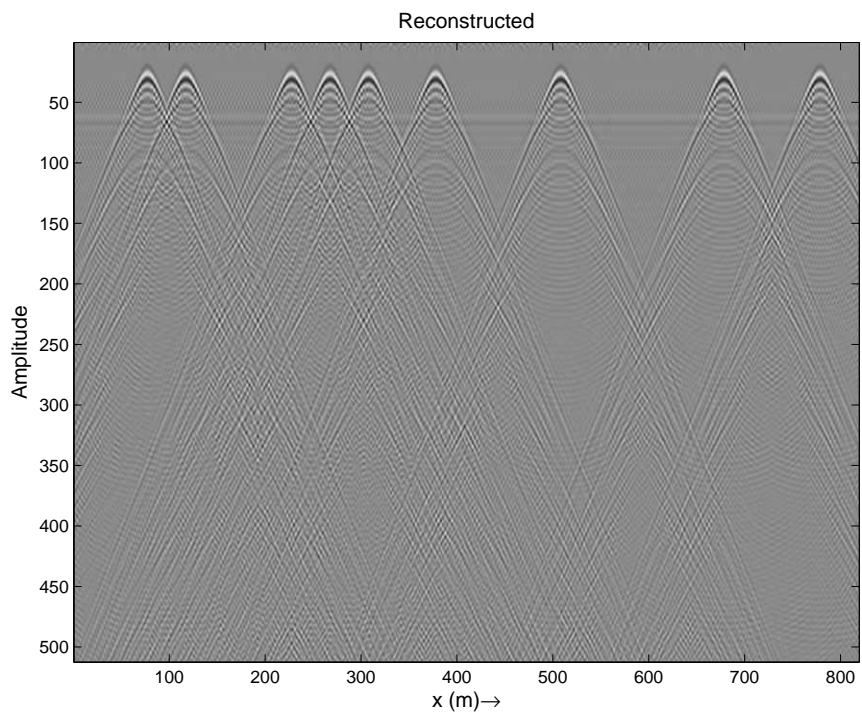
(b)

FIG. 9: Reconstruction of Hyperbolic events. a) Hyperbolic events with 20 % uniform decimation. b) Reconstructed Hyperbolic events for 20 % decimated data.